

Implementation of the Five Qubit Error Correction Benchmark

E. Knill,^{1,*} R. Laflamme,^{1,†} R. Martinez,¹ and C. Negrevergne¹

¹*Los Alamos National Laboratory, MS B265, Los Alamos, New Mexico 87545*

(Dated: October 31, 2018)

The smallest quantum code that can correct all one-qubit errors is based on five qubits. We experimentally implemented the encoding, decoding and error-correction quantum networks using nuclear magnetic resonance on a five spin subsystem of labeled crotonic acid. The ability to correct each error was verified by tomography of the process. The use of error-correction for benchmarking quantum networks is discussed, and we infer that the fidelity achieved in our experiment is sufficient for preserving entanglement.

PACS numbers: 03.67.-a, 02.70.-c, 03.65.Bz, 89.70.+c

Robust quantum computation requires that information be encoded to enable removal of errors unavoidably introduced by noise [1, 2, 3, 4, 5, 6, 7, 8]. Thus, every currently envisaged scalable quantum computer has encoding, decoding and error-correction procedures among its most frequently used subroutines. It is therefore critical to verify the ability to implement these procedures with sufficient fidelity. The experimental fidelities achieved serve as useful benchmarks to compare different device technologies and to determine to what extent scalability can be claimed.

Liquid state nuclear magnetic resonance (NMR) is currently the only technology that can be used to investigate the dynamics of more than four qubits [9, 10]. Although it is not practical to apply it to more than about ten qubits [11], it can be used to investigate the behavior of quantum networks on representative physical systems to learn more about and begin to solve the problems that will be encountered in future, more scalable device technologies. In this Letter, we describe an experimental implementation using NMR of a procedure for benchmarking the one-error correcting five-qubit code. This is the shortest code that can protect against depolarizing one-qubit errors [12, 13]. The experiment is one of the most complex quantum computations implemented so far and the first to examine the behavior of a quantum error-correcting code which protects against all one-qubit quantum noise. We discuss the principles underlying error-correction benchmarks and offer a sequence of specific challenges to be met by this and future experiments. The ultimate challenge is to demonstrate the ability to reduce the destructive effects of independent depolarizing errors. This seems to be out of reach of liquid state NMR experiments. Our experiment shows an average polarization preservation of 67% corresponding to an entanglement fidelity of .75. This easily achieves the goal of demonstrating the preservation of entanglement in principle.

The five-qubit code. A quantum error-correcting code for encoding a qubit is a two-dimensional subspace of the state space of a quantum system. In the case of interest, the quantum system consists of five qubits. The code, C_5 , can be specified as one of the 16 two-dimensional joint eigenspaces of the

four commuting operators

$$\begin{aligned} \sigma_z^{(2)} \sigma_y^{(3)} \sigma_y^{(4)} \sigma_x^{(5)} &, \quad \sigma_z^{(1)} \sigma_y^{(2)} \sigma_y^{(3)} \sigma_x^{(4)} , \\ \sigma_y^{(2)} \sigma_z^{(3)} \sigma_z^{(4)} \sigma_z^{(5)} &, \quad \sigma_x^{(1)} \sigma_z^{(2)} \sigma_x^{(3)} \sigma_z^{(4)} . \end{aligned} \quad (1)$$

Here, $\sigma_x^{(k)}, \sigma_y^{(k)}, \sigma_z^{(k)}$ are the Pauli spin operators acting on qubit k . This is an instance of a stabilizer code [14, 15], and the fact that it can be used to correct any one-qubit error is due to the property that every product of one or two Pauli operators acting on different qubits anticommutes with at least one of the operators in Eq. (1).

A typical application of a quantum error-correcting code is to protect a qubit's state in a noisy quantum memory. As implemented in our experiment, the procedure begins with qubit 2 containing the state to be protected and *syndrome* qubits 1, 3, 4, 5 in the initial state $|1\rangle$. A unitary *encoding* transformation is applied to map the two-dimensional input state space to the subspace of the code C_5 . In the application, the five qubits are then stored in the noisy memory. In our experiment, we explicitly applied one of the correctable error. The information is retrieved by first applying the inverse of the encoding transformation to *decode* the state. The properties of the code guarantee that if the error was a Pauli operator acting on one of the qubits, which one occurred is reflected in the state of the syndrome qubits. To complete the process, conditional on the syndrome qubits' state, it is necessary to *correct* the state of qubit 2 by applying a Pauli operator. Quantum networks for encoding, decoding and error-correction are shown in Fig.1.

Benchmarking quantum codes.

The purpose of a benchmark is to compare the performance of different devices on the same task. Since quantum codes will be used to maintain information in future quantum computing devices, they are excellent candidates for benchmarking the reliability of proposed quantum processors. A basic quantum code benchmark consists of a sequence of steps that implement encoding, evolution, decoding and error-correction networks. In the simplest cases, the steps are applied to one qubit's state using several ancilla qubits for the intermediate steps. An experimental implementation measures the reliabil-

ity (see below) with which the qubit’s state is processed. It is necessary to include a means for verifying that a code with the desired properties was indeed implemented. For error-correcting and for stabilizer codes, this can be done by inserting 180° pulses applied to individual qubits in the evolution step and observing their effect on the output. In this case, the verification relies on the assumption that such pulses can be reliably implemented, a property that needs to be independently verified.

To allow for unbiased comparison of devices, the reliability measurement and the verification steps of the benchmark need to be standardized. There are many different ways of quantifying reliability. The best known such measure, *fidelity*, is based on the geometry of the state space. If the input state is $|\psi\rangle$ and the output density matrix is ρ , then the fidelity of the output is given by $F(|\psi\rangle, \rho) = \langle\psi|\rho|\psi\rangle$. This can be seen to be the probability of measuring $|\psi\rangle$ in a measurement which distinguishes this state from the orthogonal states. In our case we are interested in an arbitrary state of one qubit. One quantity of interest would be the worst case pure state fidelity, which minimizes the fidelity of the implemented benchmark over pure input states. However, an easier to use quantity is the *entanglement fidelity* F_e [16], the fidelity with which a Bell state on the qubit and a perfect reference qubit is preserved. Entanglement fidelity does not depend on the choice of Bell state and has the property that $F_e = 1$ if and only if the process perfectly preserves every input state. To avoid experimentally implementing the reference qubit, F_e can be determined from the fidelities of pure states. Define $|\pm\rangle = (|0\rangle \pm |1\rangle)/\sqrt{2}$ and $|\pm i\rangle = (|0\rangle \pm i|1\rangle)/\sqrt{2}$ (the eigenstates of σ_x and σ_y , respectively). Let F_s be the fidelity of the process for input $|s\rangle$. Then

$$F_e = (F_0 + F_1 + F_+ + F_- + F_{+i} + F_{-i})/4 - 1/2. \quad (2)$$

We advocate the use of entanglement fidelity as the standard reliability measure to be given when describing the results of a quantum benchmark involving processing of a quantum bit.

The standard verification procedure for a quantum code benchmark needs to be such that sufficiently high fidelity cannot be achieved without having implemented a code with the desired properties. For codes defined as the common eigenspace of a commuting set of products of Pauli operators (stabilizer codes), it is in principle enough to verify that applying a product P of Pauli operators during the evolution has the expected effect on the output, namely that it differs from the input by the application of a Pauli operator $\sigma(P)$ determined by the code and the applied product. A single fidelity measure may be obtained by applying $\sigma(P)$ to the output and by averaging the resulting entanglement fidelities over all P . To make this procedure experimentally feasible, one may randomize the choice of P and use statistical methods to estimate the desired average.

For benchmarks involving a quantum error-correcting code, the emphasis is on having corrected the set of errors \mathcal{E} for which it was designed, and verification involves applying the errors in \mathcal{E} during the evolution and observing the extent to

which they are indeed corrected. Ideally, the errors occur naturally in the course of evolution, and one would like to see that information is preserved better by encoding it. In order to investigate the code in a controlled way, it is easier to apply different errors explicitly and observe the effect on the reliability of the process. The experiment described here involves measuring the entanglement fidelity for each of the one-qubit Pauli operators applied during the evolution.

When implementing a benchmark, it is useful to have some goals in mind. Each goal implies the demonstration of a non-trivial result. For benchmarks involving codes designed to correct independent errors on qubits, we offer a sequence of four such goals depending on how well the implementation succeeds at protecting against various error models. Most involve comparing the entanglement fidelity for two situations involving a specific error process \mathcal{E}_i . In the first, the information is stored in any one of the qubits, giving an optimum $F_{e,1}(\mathcal{E}_i)$. In the second, the information is stored by using the implemented code, giving an experimentally determined $F_{e,C}(\mathcal{E}_i)$. Numerical goals for $F_{e,C}(\mathcal{E}_i)$ are given under the assumption that the implementation induces depolarizing noise. The goals are: 1. Improvement where \mathcal{E}_1 is depolarization of each qubit with some probability p . For C_5 under the assumption that the error behavior is identically depolarizing (quantified by F_{e,C_5}) for each possible Pauli-product error during the evolution, this requires $F_{e,C_5} > 0.97$, giving an improvement when $p = 0.08713$. See Fig. 2. 2. Improvement where \mathcal{E}_2 is the process that first randomly chooses a qubit and then depolarizes it. For our code this requires $F_{e,C_5}(\mathcal{E}_2) > .85$. 3. Preservation of some entanglement for \mathcal{E}_2 . This requires $F_{e,C}(\mathcal{E}_2) > .5$ [12]. 4. Improvement in the presence of the *demonic* error process \mathcal{E}_4 that, knowing the method for storing the qubit, chooses the worst possible one-qubit depolarizing error and applies it. In this case we need $F_{e,C}(\mathcal{E}_4) > .25$. One of the ultimate goals might be to demonstrate that the code can be implemented sufficiently well to permit preservation of information by means of concatenation.

Experimental implementation. We used ^{13}C labeled trans-crotonic acid (Fig. 3) synthesized as described in [17], but with deuterated acetone as a solvent. A standard 500 MHz NMR spectrometer (DRX-500 Bruker Instruments) with a triple resonance probe was used to run the experiments. The five spin 1/2 systems used for the code are the methyl group (M), C1, C2, C3 and C4. The methods of [17] were used to prepare the methyl group as an effective spin 1/2 system and to initialize the labeled pseudo-pure state $1\sigma_z 11111$ on all active nuclei. Here, $\mathbf{1} = |1\rangle\langle 1|$ and the last two nuclei are H1 and H2. The selection method was based on gradients, and the pseudo-pure state was subjected to a “crusher” gradient. To absolutely guarantee the pseudo-pure state, more randomization is required (see [17]) but we did not implement this. H1 and H2 were not used and were only affected by some hard pulse refocusing on the protons. The state of H1 and H2 (up or down) induces an effective frequency shift on the other nuclei depending on the coupling constants and was compen-

sated for in phase calculations. To greatly reduce the effect of radio frequency (RF) inhomogeneity, we used the nutation based selection scheme of [17], applied to both the proton and the carbon transmitters. The quantum networks of Fig. 1 were directly translated to pulse sequences, again using the methods described in [17]. The only significant use of manual intervention was to place the refocusing pulses. The evolution period between encoding and decoding was carefully isolated from both the preceding and the following pulses: It implemented the identity unitary operator, or one of the one qubit 180° rotations by refocusing the molecule’s internal Hamiltonian and applying an extra inversion or by shifting the phase by 180° . The qubit’s output state appeared on C1 at the end of the experiment. The peak group associated with C1 was observed in each experiment. Spectra were analyzed by comparing the spectrum of the pseudo-pure state $1\sigma_x 11111$ to the output, using the knowledge of the peak positions and shapes to compute relative intensities and phases. No phase adjustment was made after phasing the pseudo-pure state spectrum. This was possible since the relative phase is recomputed by the pulse compiler and integrated into the acquisition.

We performed one experiment for each of the 16 possible evolutions with one-qubit or no Pauli error, each of the three initial states σ_x , σ_y or σ_z on C1, and each of three observations (no pulse, 90° X pulse, or 90° Y pulse) on C1. This resulted in a total of 112 experiments, each of which was repeated sufficiently often to get better than 8% error in the inferred state of C1. For each evolution E and input σ_u , we determined the amount of signal $P(e, u)$ in the correct direction in the output relative to the input signal. This requires “tracing out” the other spins, which was done by adding the intensities of each peak in the C1 spectrum that is associated with the 11 state on $H1$ and $H2$. (The spectrum of C1 resolves all its couplings.) Thus, except for noise, $-1 \leq P(E, u) \leq 1$. Under the assumption that input 1111111 results in no observable signal, the entanglement fidelity for a given evolution e is given by $F_e(E) = (P(E, x) + P(E, y) + P(E, z) + 1)/4$. We did not verify the assumption in this experiment, but note that it has been verified in related experiments [18], and could be enforced by modifying the process with random pairs of canceling 180° pulses before and after the implemented pulse sequence. This would also enforce the depolarizing noise model for the implementation while preserving the observed polarization.

Results. Typical spectra compared to the spectrum of the input pseudo-pure state are shown in Fig. 4. The relative polarization after the error-correction procedure in the correct output state varies between 48% and 87%. The distribution is shown in Fig. 5. The inferred entanglement fidelity for goals 2 and 3 is $F_{e,C}(\mathcal{E}_2) = .75$, with an estimated error of less than .02. Thus we clearly met goal 3.

The reduction in polarization is due to thermal relaxation, incompletely refocused couplings (part of the pulse compiler’s optimization trade-offs), pulse errors due to non-ideal implementation of 180° and 90° pulses, and RF inhomogeneity (less than 2% after our selection procedure). Most of the

error is explained by the known relaxation times, suggesting that this is what limits the fidelities that can be attained using liquid state NMR. We note that the estimated phase relaxation times of well over a second are high when compared to those of nuclei in other molecules used in NMR quantum information processing experiments to date.

Discussion. Benchmarking quantum devices for quantum information processing is crucial both for comparing different device technologies and for determining how much control over a device is achievable and how to best achieve it. Given the need for and difficulty of achieving robust quantum control, we advocate the use of quantum coding benchmarks to determine the fidelity of the implementation of standard, verifiable processes. Unlike the experimentally implemented versions (up to 5 qubits) of the popular quantum searching and order-finding algorithms [19, 20, 21, 22, 23, 24], quantum codes offer a rich source of complex and verifiable quantum procedures required in currently envisioned quantum computer architectures. Liquid state NMR has been used to implement several interesting, small quantum codes [18, 25], and a seven qubit cat-state benchmark [17]. In this letter, we have given specific goals for benchmarks involving error-correction and, for the first time, implemented a one-qubit error-correcting quantum code. The fidelity achieved is well above what is needed to demonstrate preservation of entanglement in the presence of a non-trivial error-model. It is unlikely that the goal of showing improvement in error-correcting independent depolarizing errors is achievable with liquid state NMR. A device that achieves this challenging goal will be well on the way toward realizing robustly scalable quantum computation.

Acknowledgments. Supported by the Department of Energy (contract W-7405-ENG-36) and by the NSA. We thank the Stable Isotope Resource for providing equipment and support. We thank Ryszard Michalczyk, Brian MacDonald, Cliff Unkefer and David Cory for their help.

* Electronic address: knill@lanl.gov

† Electronic address: laflamme@lanl.gov

- [1] P. W. Shor, Phys. Rev. A **52**, 2493 (1995).
- [2] A. Steane, Proc. R. Soc. Lond. A **452**, 2551 (1996).
- [3] E. Knill and R. Laflamme, Phys. Rev. A **55**, 900 (1997).
- [4] P. W. Shor, in *Proceedings of the 37th Symposium on the Foundations of Computer Science (FOCS)* (IEEE press, Los Alamitos, California, 1996), pp. 56–65.
- [5] D. Aharonov and M. Ben-Or, in *Proceedings of the 29th Annual ACM Symposium on the Theory of Computation (STOC)* (ACM Press, New York, New York, 1996), pp. 176–188.
- [6] A. Y. Kitaev, Russian Math. Surveys **52**, 1191 (1997).
- [7] E. Knill, R. Laflamme, and W. H. Zurek, Science **279**, 342 (1998).
- [8] J. Preskill, Proc. R. Soc. Lond. A **454**, 385 (1998).
- [9] D. G. Cory, A. F. Fahmy, and T. F. Havel, Proceedings of the National Academy of Sciences of the United States of America **94**, 1634 (1997).

- [10] N. A. Gershenfeld and I. L. Chuang, *Science* **275**, 350 (1997).
- [11] W. S. Warren, *Science* **277**, 1688 (1997).
- [12] C. H. Bennett, D. P. DiVincenzo, J. A. Smolin, and W. K. Wootters, *Phys. Rev. A* **54**, 3824 (1996).
- [13] R. Laflamme, C. Miquel, J.-P. Paz, and W. H. Zurek, *Phys. Rev. Lett.* **77**, 198 (1996).
- [14] D. Gottesman, *Phys. Rev. A* **54**, 1862 (1996).
- [15] A. Calderbank, E. Rains, P. Shor, and N. Sloane, *Phys. Rev. A* **78**, 405 (1997).
- [16] B. Schumacher, *Phys. Rev. A* **54**, 2614 (1996).
- [17] E. Knill, R. Laflamme, R. Martinez, and C.-H. Tseng, *Nature* **404**, 368 (2000).
- [18] D. G. Cory, W. Maas, M. Price, E. Knill, R. Laflamme, W. H. Zurek, T. F. Havel, and S. S. Somaroo, *Phys. Rev. Lett.* **81**, 2152 (1998).
- [19] J. A. Jones and M. Mosca, *J. Chem. Phys.* **109**, 1648 (1998).
- [20] J. A. Jones, M. Mosca, and R. H. Hansen, *Nature* **392**, 344 (1998).
- [21] I. L. Chuang, L. M. K. Vandersypen, X. Zhou, D. W. Leung, and S. Lloyd, *Nature* **393**, 143 (1998).
- [22] I. L. Chuang, N. Gershenfeld, and M. Kubinec, *Phys. Rev. Lett.* **80**, 3408 (1998).
- [23] R. Marx, A. F. Fahmy, J. M. Myers, W. Bermel, and S. J. Glaser, *Realization of a 5-bit NMR quantum computer using a new molecular architecture* (1999), quant-ph/9905087.
- [24] L. M. K. Vandersypen, M. Steffen, G. Breyta, C. S. Yannoni, R. Cleve, and I. L. Chuang, *Phys. Rev. Lett.* **85**, 5452 (2000).
- [25] D. Leung, L. Vandersypen, X. L. Zhou, M. Sherwood, C. Yannoni, M. Kubinec, and I. Chuang, *Phys. Rev. A* **60**, 1924 (1999).
- [26] S. S. Somaroo, D. G. Cory, and T. F. Havel, *Phys. Lett. A* **240**, 1 (1998).

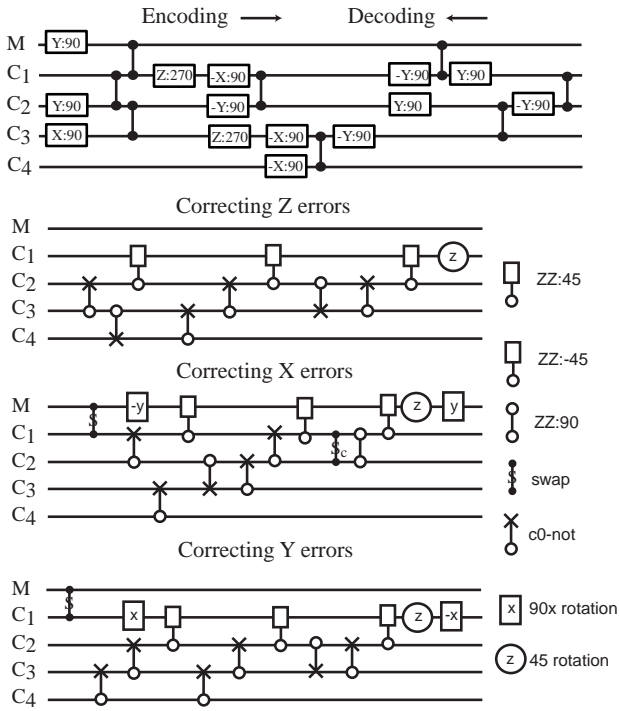


FIG. 1: Networks for the 5-qubit code. Top: The encoding network using 90° rotations. Except for refocusing required to eliminate unwanted couplings, these are directly implementable with pulses. The decoding network is the inverse of the encoding network. Bottom: The three steps of the error-correction procedure, which implements a rotation on C1 conditional on the syndrome state. The controlled operations can be translated to sequences of 90° rotations using standard quantum network methods [26].

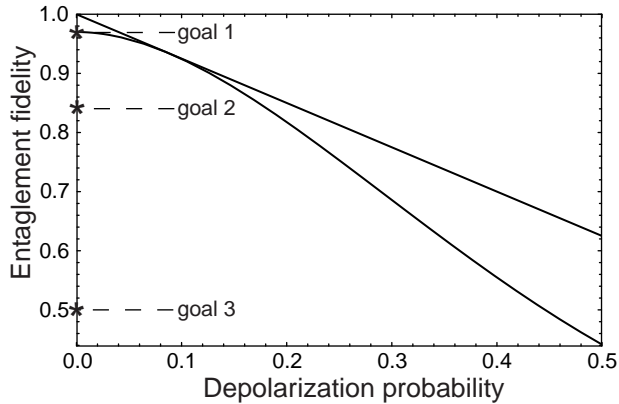


FIG. 2: Entanglement fidelities for independent depolarization. The fidelities for an unencoded qubit (straight line) and a qubit encoded with C_5 are shown as a function of the depolarization probability. The implementation of the code is assumed to have an additional error that is syndrome independent with depolarization probability .97. The first three fidelity benchmarking goals are indicated.

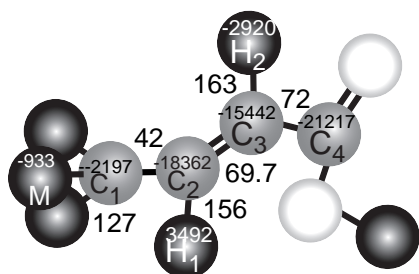


FIG. 3: Trans-crotonic acid. The chemical shifts and nearest neighbor couplings are shown.

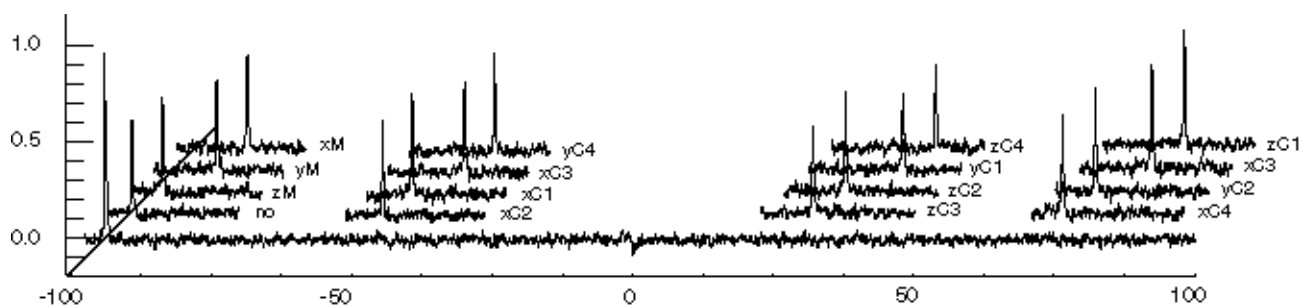


FIG. 4: Experimental input and output spectra. The reference spectrum for the pseudo-pure input is at the bottom, and partial spectra for each one-qubit error are shown above it using the same scale. The labels indicate which error on which nucleus was applied. One peak is observed for each possible error input. Its position corresponds to the error syndrome. Its phase reflects the error correction procedure and corresponds to the input state up to a small error. Signal in the wrong locations or phase was consistently small and comparable to the estimated noise.

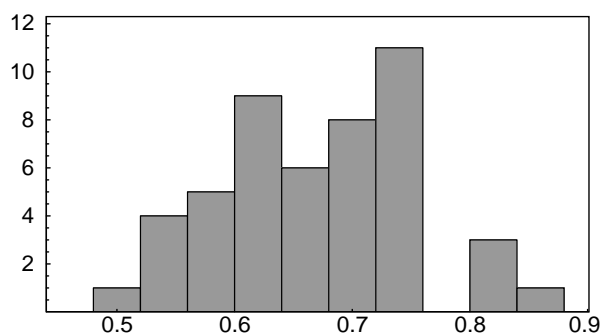


FIG. 5: Distribution of relative polarizations. There are a total of 48 polarization measurements. Each bar represents the number of measurements with relative polarization in the bar's interval. The distribution strongly suggests some syndrome-dependent effects on the implementation error.